JPE 6-3-7

Detection of Broken Bars in Induction Motors Using a Neural Network

M. Moradian*, M. Ebrahimi†**, M. Danesh** and M. bayat**

*Dept. of Electrical Eng., Isfahan University of Tech., Isfahan, Iran
†**Dept. of Eng., Islamic Azad University of Najafabad, Isfahan, Iran

ABSTRACT

This paper presents a method based on neural networks to detect the broken rotor bars and end rings of squirrel cage induction motors. At first, detection methods are studied, and then traditional methods of fault detection and dynamic models of induction motors by using winding function model are introduced. In this method, all of the stator slots and rotor bars are considered, thus the performance of the motor in healthy situations or breakage in each part can be checked. The frequency spectrum of current signals is derived by using Fourier transformation and is analyzed in different conditions. In continuation, an analytical discussion and a simple algorithm are presented to detect the fault. This algorithm is based on neural networks. The neural network has been trained by using information of a 1.1 KW induction motor. This system has been tested with a different amount of load torque, and it is capable of working on-line and of recognizing all normal and ill conditions.

Keywords: squirrel cage, induction motor, rotor fault, neural network

1. Introduction

Most faults in electrical motors cause production to stop or to be reduced and even cause other machines to break. There are several methods for detecting broken rotor bars and end rings of squirrel cage induction motors[1-8]. Each of these methods has advantages and disadvantages and depending on the application and situation of the motor, each can use any of these methods or a combination of them. MCSA method is very applicable, because [2]:

1) Stator winding is used as a finder winding

2) This method is independent of other faults

In this method, breakage in bars or end ring causes the existence of frequency components around the main component of the stator current. Therefore these components are used for detecting faults. For this objective, after sampling of current, by using FFT and with the hanning window, the value and amplitude of the frequency component is calculated and variations of these components are used to detect fault. Due to disturbances in producing bars in motors, rotor bars become unbalanced. This causes minor harmonic components to be used, since in real motors, it is necessary to assume a limit boundary between unhealthy and healthy motors. The existence of harmonic components resulting from problems such as vibrations of mechanical load is very important, and it should be separated from the fault component. Therefore, using an intelligent system is unavoidable in detecting faults [1].

Recent references show that the Artificial Neural Network (ANN) has very successful applications in fault recognition, control, and signal processing. These networks are capable of fault recognition in motors that have nonlinear variables. The most important advantage of this

Manuscript received February. 2, 2005; revised May. 23, 2006
†Corresponding Author: mebrahim@cc.iut.ac.ir
Tel: +202-331-0512, Fax:+202-335-1631, Islamic Azad Univ
*Dept. of Electrical Eng., Isfahan University of Tech
**Dept. of Eng., Islamic Azad University of Najafabad

method is fast signal processing in an on-line mode since all complex calculations refer to the training step, which is in off-line mode [9].

In addition, ANNs do not need a rigorous mathematical model for fault detecting and they are very flexible in problem solving[10]. In addition, ANN is much cheaper than frequency monitoring method and particle analysis method.

In this paper, a neural network is suggested to detect broken bars and end rings. This network will be able to recognize the situation of rotors, like health or breakage, and a number of broken bars, by receiving the result data from frequency spectrum of the stator current.

This paper explains the broken rotor fault and motor modeling by using a winding function model. In this model, it is possible to model broken bars and the end ring. It explains the effect of breakage on different signals of the motor such as current, and then explains how to process the current signal, and use neural network for fault detection, and then the practical result is presented.

2. Modeling Induction motor, using winding function method

At first, it is necessary to specify the objectives. In this discussion, it is necessary to model each bar and each end ring separately. To achieve this objective, a dynamic model based on winding function is presented[11]. In this method, the rotor that includes Nr bar is regarded as a circuit with Nr loop and each loop includes two bars and two end ring junctions. A 3-phase system is assumed for stator and the effect of stator slots and distributed winding is assumed, too. Stator and rotor circuit parameters and their dimensions are: rotor resistance matrix Rrr [Nr × Nr], rotor inductance matrix Lrr[Nr × Nr], stator resistance matrix Rss [3 × 3], stator inductance matrix Lss [Nr × Nr] Mutual inductance of stator and rotor is shown by Lsr [3 × Nr] matrix. All of these matrices have been calculated by winding function methods.

2.1 Calculation of inductances based on winding function method

The winding function method is used to calculate inductances of the induction motor model [11].

Mutual inductance between winding x,y is calculated by integrating the result of multiplying N(φ) turn function of one winding by n(φ) winding function of another winding in limitation of [0,2π]. The result of this integral is multiplied by a constant coefficient that depends on the physical specification:

$$L_{xy} = \frac{\mu_0 rl}{g} \int_0^{2\pi} N_x(\varphi)\cdot n_y(\varphi) d\varphi \qquad (1)$$

In this equation, g is the length of air gap, l is the length of machine shaft, r is the average radius of air gap, and φ is the angular position. Motor inductances are calculated by using this method. This motor has 44 bars in the rotor and 36 slots in the stator and its winding is one layer and diagonal. (The other characters of this motor are presented in appendix A). For example, L_{ar1} mutual inductance of phase (a) with the first loop of rotor L_{ar1} is:

$$L_{ar_1} = \frac{\mu_0 rl}{g}\cdot\frac{-N}{6}\left(-2\theta_{rm} + \frac{45\pi}{22}\right) \qquad (2)$$

Where θ_{rm} is the angular position of the rotor

Also the mutual inductance of phase a and b is calculated as:

$$L_{ab} = \frac{30\, rl}{g} \times \frac{-N^2\pi}{6} \qquad (3)$$

The mutual inductances of rotor loops have been calculated similarly. For example, the mutual inductance of the first loop and the third loop is:

$$L_{r1\,r3} = \frac{20\, rl}{g} \times \frac{-2\pi}{(44)^2} \qquad (4)$$

This method has been used for calculating the magnetizer inductance of a coil. For this purpose, it is necessary to multiply the turn function by the winding function of the same coil, and this result is integrated in one cycle. For example, the magnetizer inductance of x winding is:

$$L_{mx} = \frac{\mu_0 rl}{g} \int_0^{2\pi} N_x(\varphi)\cdot n_x(\varphi) d\varphi \qquad (5)$$

According to equation (5), the magnetizer inductance of each phase of the stator and the magnetizer inductance of rotor loops have been calculated as:

$$L_{ms} = \frac{30rl}{g} \times \frac{65\pi N^2}{16z} \tag{6}$$

$$L_{mr} = \frac{30rl}{g} \times \frac{86\pi}{(44)^2} \tag{7}$$

2.2 Dynamic equation of induction motor

Voltage and flux equation are Shown below [12]:

$$V_s = R_{ss} I_s + \frac{d\lambda_s}{dt} \tag{8}$$

$$0 = R_{rr} I_r + \frac{d\lambda_r}{dt} \tag{9}$$

$$\lambda_s = L_{ss} I_s + L_{sr} I_r \tag{10}$$

$$\lambda_r = L_{rs} I_s + L_{rr} I_r \tag{11}$$

Where V_s, I_s, λ_s are voltage, current and flux vectors of the stator and I_r, λ_r are current and flux vectors of the rotor.

Flux and current equations are as below:

$$\lambda = L I \tag{12}$$

$$I = L^{-1} \lambda \tag{13}$$

Where λ is the flux vector and I is the current vector of the motor. According to electrical torque equation and mechanical equation, the value of speed and angular position has been calculated as below:

$$T_e = I_s^T \left(\frac{\partial L_{sr}}{\partial \theta_{rm}}\right) I_r \tag{14}$$

$$T_e - T_l = J \frac{d\omega_{rm}}{dt} \tag{15}$$

$$\omega_{rm} = \frac{d\theta_{rm}}{dt} \tag{16}$$

Where T_e is the electrical torque, T_l is the mechanical load torque and ω_{rm} is the angular speed of rotor.

According to value of inductances that are calculated in each time, the value of the flux, torque, speed and angular position, have been calculated.

3. Current signal analysis method to detect broken rotor bars

When the breakage occurs in rotor bars or end rings, the rotor circuit and its current will be unbalanced. Therefore, currents of this circuit can be separated in two components, and these currents create two rotating fields with $\pm sf_s$ frequencies in opposite directions in the air gap. These fields cause components to create in the air gap flux with $\pm sf_s$ frequencies. Amplitude of these components is dependent on structural specifications and other variables of the motor. The existences of these fluxes cause components to create in the stator currents. In the other side, because of interaction between (1-2s) fs components in line current and main component of air gap flux, a distortion with $2sf_s$ frequency created in speed.

This phenomenon itself causes some other components to create in air gap field with $\pm(2k-1)sf_s$ frequencies, in speed with $2ksf_s$ frequency, in stator current with $(1\pm 2ks)f_s$ frequencies and in rotor current with $(2k-1)sf_s$ frequency.

The MCSA method is based on analyzing the variation of amplitude and frequency of sideband harmonics in stator currents [2].

4. Detection of rotor faults by Using neural network

Neural networks are highly applicable to fault detection. Many factors must be considered in designing neural networks [13,14] :

a) Network training: determining input and output variables and selection of deal data
b) Practical consideration: the network accuracy, the robustness of the network and the ability to implement
c) Network designing: the amount of input and output nodes, the amount of hidden layers and the amount of hidden nodes in hidden layers.

Determining theses parameters are based on trial and error methods, but in some cases there are some rules. For example, in the neural network with 3 layers, neurons of the hidden layer are greater than input and output neurons. If there is not enough data for training, the network will not work accurately. The objective of this paper is designing a neural network that can detect rotor breakage based on input in all conditions. Therefore, a neural network with 3 layers, a back propagation and feed forward, is suggested.

This network has 3 neurons in input layer and has 5 neurons in output layer. The network inputs are the amplitude of fundamental (a_1), amplitude of (1+2s) fs harmonic (a_u) and its frequency (f_u) in stator current spectrum. The network output shows various status of rotor i.e. normal or breakage. In each status one of the outputs is “1” and the others are “0”. The structure of this neural network is shown in figure (1). The sigmoid function is used in hidden layer neurons and this function is in the form of sigmoid hyperbolic tangent, and neurons of output layer are linear. For training of network, selections of initial weights are random and then the output is calculated based on input pattern and then these values are compared with the desired output and the amount of error is recognized and the weights are regulated based on these errors.

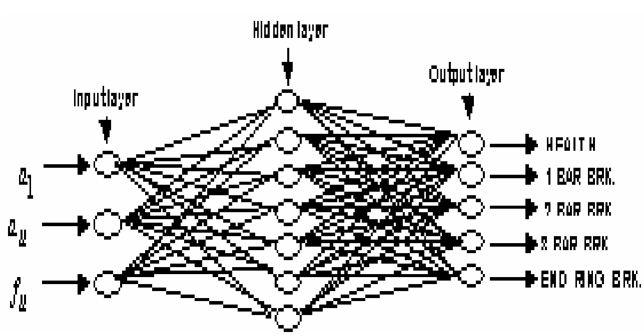

Fig. 1 Structure of neural network

5. Results of simulation

A 3 hp induction motor with parameters that are listed in appendix A is simulated. In modeling rotor breakage, the resistance of each broken section is considered as a huge number in the rotor resistance matrix. Therefore, each breakage is detected with a variation of resistance in that section. In addition, 12 N.m load torque is applied to the motor and the state of the motor is simulated in some conditions and then the frequency spectrum of stator current is earned by FFT. The frequency signature for normal status, rotor with two broken bars and broken end rings are shown in figure (2). Consider that with increasing breakage, the amplitude of (1±2ks) f_s sideband is increased.

In table (1), a part of results in analysis of frequency domain of stator current in different conditions is presented. This table includes value of load torque, steady state speed of motor, slip and amplitude of sideband harmonic.

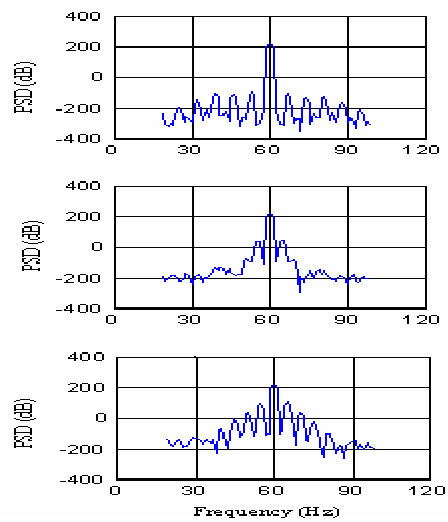

Fig. 2 Power spectral density of stator current in:
a) normal status b) rotor with two broken bars
c) rotor with broken end ring

5.1 Training and using of neural network

Sideband harmonics are used for recognizing the situation of the rotor and amplitude of these harmonics is a function of load torque and also the kind of breakage. On the other side with the addition of these frequencies, there are other natural frequencies because of rotor and stator slots, industrial environment noises and vibration of mechanical load. Since it is not possible to detect the situation of the rotor by using these frequencies, it is necessary to use a neural network. The Levenberg-Marquart function is used to train the neural network and maximum permissible error in the training step is 0.001. In continuation, the neural network was fed by the amplitude of the fundamental component of the current, as well as the amplitude and frequency of the sideband. In each case, the output of neural network has shown the status of the rotor, and the effectiveness of the system has been validated through several tests.

6. Practical results

Figure (3) shows the set that has been used for the practical test.

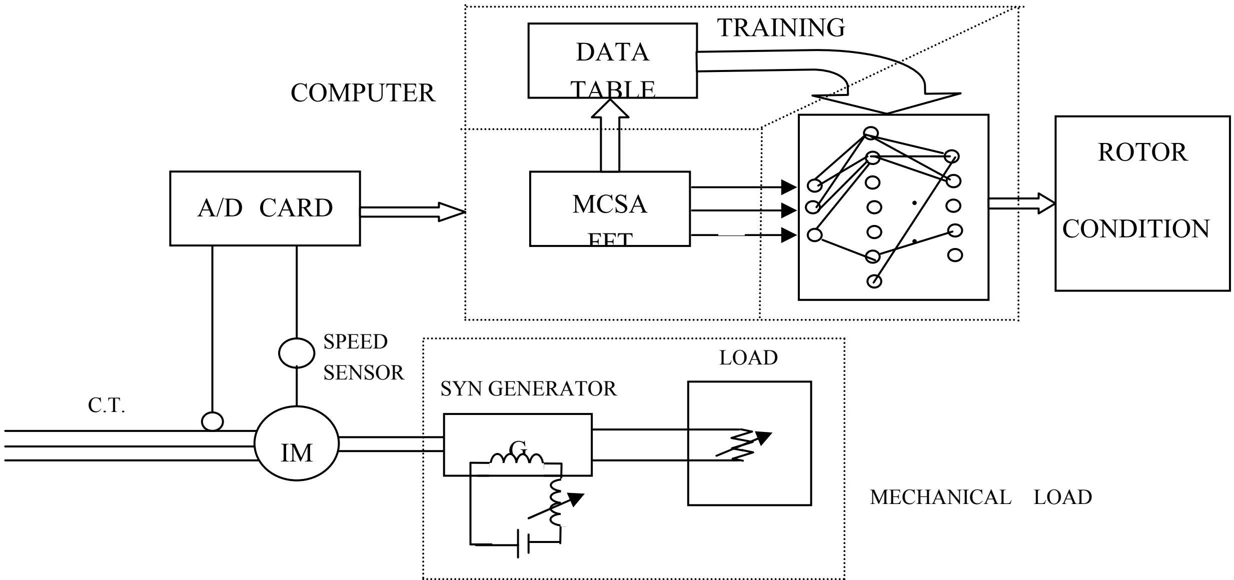

Fig. 4 Software and hardware system for broken rotor faults detection

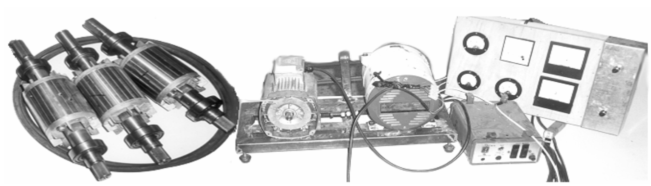

Fig. 3 Set of practical test

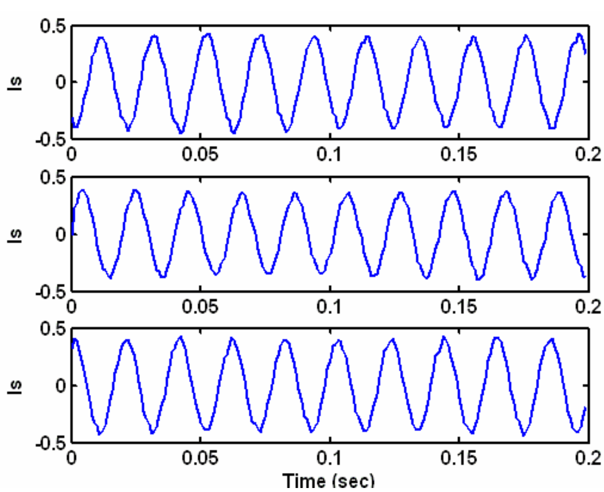

Fig. 5 Practical stator current in: a) normal status b) rotor with two broken bars c) rotor with broken end ring

This set includes a 1.1 kW squirrel cage induction motor with 36 stator slots and 28 rotor bars, together with three additional rotors, the synchronous generator that will be used as load torque, a data acquisition card and a PC.

As you see in figure (4), by running this system, current and speed are sampled and are saved in a file. Stator current are shown in figure (5) This work has been done for a normal rotor, a rotor with one broken bar, end ring broken rotor and with changing of different mechanical loads. The rotor is cut for modeling of breakage. Written software then produces the frequency signature of sampled current with FFT method. The results of frequency signature of the practical motor are shown in figure(5) between 0 to 100Hz (with normal rotor, broken end ring, and two broken bars). In the next step, the value of slip

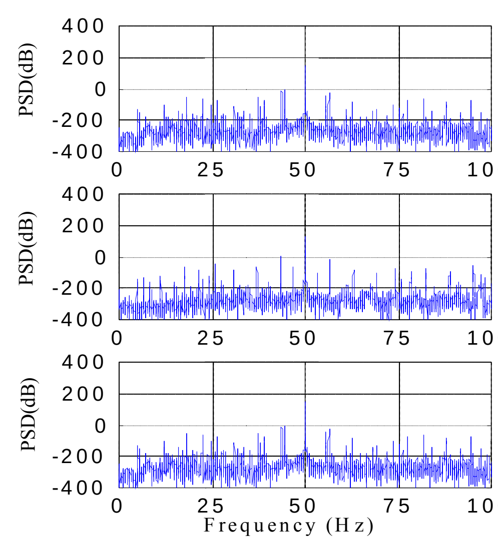

Fig. 6 Power spectral density of practical stator current in: a) normal status b) rotor with two broken bars c) rotor with broken end ri

Table 1 A part of Simulation Results

Output of neural network	Sideband frequency	Amplitude of Sideband component	Amplitude of fundamental component	condition of rotor	Load Torque
HEALTH	63.18	0	3.539	Health	75%
1 BAR BRK.	63.62	0.0208	3.872	One broken bar	83%
2 BAR BRK.	64.14	0.0568	4.237	Two broken bars	91%
3 BAR BRK.	64.72	0.1170	4.633	Three broken bars	100%
END.RING BRK.	63.67	0.1773	3.613	Broken end ring	75%

Table 2 Output of Neural Network in Different Rotor Conditions and Load Torque

Output of neural network	Sideband frequency	Amplitude of Sideband component	Amplitude of fundamental component	condition of rotor	Load Torque
HEALTH	54.07	0.031	4.048	Health	90%
2 BAR BRK.	53.00	0.280	3.158	Two broken bars	30%
END.RING BRK.	53.27	0.110	3.581	Broken end ring	60%

And the sideband frequency are determined by using measurement speed. At first, slip is computed based on s=(nsyn-nm)/nm. Then, the frequencies of sidebands are determined regarded to this slip based on (1±2s)fs. Also, using "fft" and "spectrum" instructions in MATLAB software, the power spectrum density and then amplitude of sideband components are computed. It is possible to separate the fault components from other frequency components. We can then obtain amplitude and frequency of sideband by using frequency signature.

Like table (1) another table is produced by using the information of rotor situations and value of load torques and this table has been used to train the neural network. (Table (2)) After the training step, in order to check the performance of the fault detection system, the motor has been used with different load torques. Some of these results are shown in table (2). For this setup, the trained NN correctly diagnosed the actual conditions in all of the test cases. Thus, this fault detection system shows a high level of performance.

7. Conclusion

In this paper, faults in induction motors and methods of fault detection including special broken bars or end ring faults are presented. An induction motor has been modeled based on winding function. By using this model, different signals such as speed, torque and current could be studied in different fault cases. By using simulation results and analysis of performance of the induction motor, it has been shown that in fault situations, some frequencies would be produced around the fundamental frequency. The value of the frequency and amplitude are dependent on the kind of fault and the amount of load torque. Therefore, these values have been used as a main parameter in the fault detection algorithm. In industrial applications, there are some other frequencies that are caused by motor structure, industrial environment noises and disturbances during the process of producing the motor. In these conditions, there are interferences between pieces of information that are used in the fault detection system, and it would be impossible to recognize the condition of motors easily. A neural network is a very useful method for fault detection. Therefore, the stator current and speed have been sampled in different conditions of load torque and rotor faults. The value and frequency of fundamental and sideband harmonics have been calculated. This information has been used to train the neural network.

Simulation and practical results, respectively on a 60Hz and a 50Hz induction motor, validate the effectiveness of this system of fault detection. This method is capable of working on-line and recognizing all normal and ill conditions in induction motors. For more fault conditions the amplitudes of sidebands are grown. Therefore, it seems that the recognition of fault becomes simpler.

Appendix A

Specifications of simulated motor:
3 hp, 3-Phase, 4-poles, 460 Volt, 60 Hz
Length of stator and rotor shaft = 2 ′
Width of slot = 0.12 ′
Internal diameter of stator r= 4.875 ′
Length of air gap = 0.013 ′
Number of stator slots = 36
Number of rotor bars = 44
Stator resistance = 3.7 Ω/phase
Rotor bar resistance = 50.06 μΩ
Rotor's end ring resistance = 2.6748 μΩ
Inertial moment = 0.0113 Kg m^2
Stator winding has one layer with 54 turns in each slot.

Acknowledgment

This research has been conducted as a M.S. project in Isfahan University of Technology. The Research Center of Isfahan Electricity Generation Center has provided financial support, thus the authors appreciate the assistance provided by the authorities of these departments.

References

[1] S. Nandi, "Condition monitoring and fault diagnosis of electrical machines-a review", in IEEE Thirty-Fourth IAS Meeting, vol. 1, 1999, pp. 197-204.
[2] G.B. Kliman, R.A. Koegl, "Noninvasive detection of broken rotor bars in operating induction motors" IEEE Trans. Energy Conversion, vol. EC-3, no.4, pp. 873-879, Dec. 1988.
[3] H. Meshkinkelk "Three dimensional modeling of squirrel cage induction motor with conventional rotor faults" PhD thesis; polytechnic university of technology.
[4] F. Filippetti and G. Franceschini, "A techniques in induction machines diagnosis including the speed ripple effect," IEEE-IAS Annual Meeting Conference, San Diego, Oct.6-10, 1996, pp. 655-662.
[5] F. Filippetti and G. Franceschini, "Broken bar detection in induction machines: comparison between current spectrum approach and parameter estimation approach," Proceedings of the IEEE-IAS Annual Meeting Conf, Denver, Colorado , USA, vol. 1, 1994, pp. 95-102.
[6] A. Bardour and W.T. Thomosn, "Finite element study of rotor slot designs with respect to current monitoring for detecting static air gap eccentricity in squirrel-cage induction motor," Proceedings of the IEEE-IAS Annual Meeting Conference, New Orleans, LA, Oct. 5-9, 1997, pp. 112-119.
[7] K. Kyusung, "Induction motor fault diagnosis based on neuro predictors and wavelet signal Processing," IEEE Trans. Mechatronics, vol. 7, no. 2, pp. 201-219, 2002.
[8] H. Masoud, "Pattern recognition-A technique for induction machines rotor broken bar detection," IEEE Trans. Energy Conversion, vol. 16, no. 4, 2001.
[9] M. Rokonuzzaman and M.A. Ranman, "Neural network based incipient fault detection of induction motors," IEEE-IAS, 1995, pp. 199-202.
[10] P.V. Goode, Neural Fuzzy systems for incipient fault detection in induction motors," IEEE-IECON, vol. 1, 1993, pp. 332-337.
[11] H.A. Toliyat, " Analysis of concentrated winding induction and reluctance motors for adjustable speed drive applications," Ph. D. dissertation, University of Wisconsin Madison, Madson, Wisconsin, USA, February 1991.
[12] H.A. Toliyat and T.A. Lipo, "Transient analysis of cage induction machines under stator, rotor bar and end ring fault," IEEE Trans on EC., vol. 10, no. 2, pp. 241-247, June, 1995.
[13] F. Filippetti and G. Franceschini, "Neural networks aided on-line diagnostics of induction motor rotor faults", IEEE Trans. On Industry Applications, vol. 31, no. 4, pp. 892-899, Jul. Aug., 1995.
[14] M.Y. Chow, "Design considerations for a motor fault detection artificial neural network," IEEE, Industrial Electronics, Control, Instrumentation, and Automation, Conference on Nov. 1992, vol. 3, pp. 1455-1459.

Mohamadreza Moradian was born in Isfahan, Iran in 1975. He received his B.S. and M.S. degrees in electrical engineering from Isfahan University of Technology, Iran, in 1998 and 2000, respectively. Since 2001, he has been a faculty member in the Department of Electrical Engineering in Azad Islamic University of Najafabad, Iran. His research interests are in the areas of modeling and control of ac motors.

Mohammad Ebrahimi was born in Isfahan, Iran, in 1958. He received his B.S. and M.S. degrees in electrical engineering from Tehran University in 1984 and 1986, respectively, and received his Ph.D. degree in 1996. He is an assistant professor in the department of electrical engineering, Isfahan University of Technology, Isfahan, Iran. His research interests include application of artificial intelligence based electrical machines and derivatives, sensorless electric motor drive, condition monitoring and fault diagnosis of electric machinery, simulation techniques in electrical machines and derivatives, efficiency optimization and energy saving.

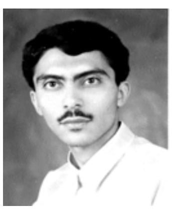

Mohammad Danesh received the B.S. and M.S. degrees in control engineering in 1997 and 1999, respectively, where he is currently working as a Ph.D. student. His research interests include robotics, intelligent systems and adaptive control. He is a member of Iranian Association of Electrical and Electronic Engineering (IAEEE) and also a member of the Institute of Electronics, Information and Communication Engineers (IEICE).

Mohammad Bagher Bayate was born in Tehran, Iran in 1964. He received the B.S. in electrical engineering from Amir Kabir University, and M.S. degree from Tarbiat Modarres University in 1989 and 1993 respectively. Since 1995 he has been with R&D Department of SABA Co. His research interests are in the area of power electronics and industrial automation.